Radovan Jiřík

QUANTITATIVE PERFUSION IMAGING USING ULTRASONOGRAPHY AND MRI

BRNO UNIVERSITY OF TECHNOLOGY

Faculty of electrical engineering and communication

Department of biomedical engineering

Ing. Radovan Jiřík, Ph.D.

QUANTITATIVE PERFUSION IMAGING USING ULTRASONOGRAPHY AND MRI

KVANTITATIVNÍ ZOBRAZOVÁNÍ PERFUZE POMOCÍ ULTRASONOGRAFIE A MRI

SHORT VERSION OF HABILITATION THESIS
FIELD: BIOMEDICAL ENGINEERING

Vysoké učení NAKLADATELSTVÍ
Technické VUTIUM
V Brně

BRNO 2022

Key Words

Perfusion imaging, pharmacokinetic modeling, ultrasonography, magnetic resonance imaging.

Klíčová slova

Zobrazování perfuse, modelování farmakokinetiky, ultrasonografie, zobrazování magnetickou resonancí.

Deposition Location / Místo uložení

The habilitation thesis is available at the Department of Science and International Relations, Faculty of Electrical Engineering and Communication, Brno University of Technology.

Habilitační práce je uložena na Vědeckém a zahraničním oddělení Fakulty elektrotechniky a komunikačních technologií, VUT v Brně.

CONTENTS

About the author

Ing. Radovan Jiřík, Ph.D.
*1976, Czech Republic
Institute of Scientific Instruments of the Czech Academy of Sciences
Department of Biomedical Engineering, Faculty of Electrical Engineering and Communication, Brno University of Technology
E-mail: jirik@isibrno.cz, jirik@vut.cz

Education

- 1994-1999 – Master's Degree (obtained title Ing.) in Automatic, Control and Measurement in combination with Biomedical Engineering, Brno University of Technology, Brno, Czech Republic
- 1999 – Master's thesis stay at Universite Joseph Fourier, Grenoble, France (4 months)
- 1999-2004 – Ph.D. study, Department of Biomedical Engineering, Brno University of Technology, Brno, Czech Republic (Topic: Restoration and Analysis of Ultrasonic Images, supervisor: Prof. Jiří Jan)
- 2001–2002 – Ph.D. stay at University of Bergen, Norway (10 months)
- 2017 – Research stay at University of Utah, USA (5 months)

Previous and current positions

- 1995-1997 – Software development for signal and image processing (Elsyst Engineering, s.r.o., Vyškov)
- 1997-1998 – Hardware / software development for continuous blood cleaning devices (Skála OK, s.r.o., Brno)
- 1998-2001 – Design of a dental R.T.G. control unit – hardware / software (BMT Brno, a.s., Brno)
- 2004-present – Teacher and research assistant, Dept. of Biomedical Engineering, Brno University of Technology
- 2008-present – Senior research position, Institute of Scientific Instruments of the Czech Academy of Sciences, Brno

- 2012-2015 – Senior research position, International Clinical Research Centre, St. Anne's University Hospital (FNUSA-ICRC)

Project leader
- 3 mobility projects of the Czech Academy of Sciences and the German Academic Exchange Service (AVČR/DAAD)
- 4 standard projects of the Czech Science Foundation (GAČR)

Past and current teaching activities
- Signal and image processing (laboratory classes)
- Modeling of biological systems (lectures, laboratory classes)
- Systems biology (lectures, laboratory classes)
- Medical imaging systems (MRI) (lectures, laboratory classes)
- Supervision of 8 bachelor, 14 master and 4 Ph.D. defended projects

INTRODUCTION

The word *perfusion* describes, in general, the passage of a fluid through natural channels in a tissue. In the most cases, this general meaning is narrowed to blood, and perfusion is understood as circulation of blood through tissues. The topic of this habilitation thesis, perfusion imaging, relates to methods providing parameters describing perfusion. Examples of such perfusion parameters are blood flow, blood volume, vessel-wall permeability expressed per unit mass or unit volume of tissue. These parameters describe the physiological state of the tissue on the microvascular level. They are important biomarkers in many clinical and biological applications. Perfusion imaging is important especially in oncology, where it provides a noninvasive way to early identification of tumor types. Furthermore, it provides an early-stage insight into the efficacy of tumor treatment since the reaction to tumor treatment is much faster on the microvascular level expressed by perfusion parameters (days to weeks) than on the macroscopic level expressed by standard anatomical images (months). That means that perfusion imaging can give a substantially earlier evaluation of the treatment process than the standard criteria based on measurements of tumor volume from anatomical images. Hence, such early evaluation of the treatment response is a key to qualified decisions on the treatment strategy, which can ultimately prolong or safe lives and substantially decrease health-care costs.

Perfusion imaging is a valuable tool also in preclinical research, especially in testing of new treatment strategies on animals (e.g. antiangiogenic treatment in oncology) and drug-delivery paths (e.g. drug delivery through the blood brain barrier in neurology).

However, in many applications, current perfusion imaging methods are not sufficiently reliable for routine clinical use, where they remain mostly at the experimental level, although their principles have been known for several decades.

The topic of perfusion imaging is a unique multidisciplinary field. It combines the physics of the image acquisition processes, knowledge of physiology and mathematics needed for understanding and modeling of the perfusion process, as well as the field of signal and image processing needed for image reconstruction and image pre- and post-processing. An important part of pharmacokinetic-model fitting in perfusion imaging is also understanding of approaches to inverse problem solving. Furthermore, identification of relevant applications for perfusion imaging and management of the examined subjects (patients, animals), as well as interpretation of the results often requires medical, veterinarian or biological expertise. This multidisciplinary character of perfusion imaging is one of the reasons of the author's enthusiasm

for this field. The combination of the above mentioned disciplines overlaps very well with the curriculum taught at the Department of Biomedical Engineering at Brno University of Technology. The author has introduced perfusion imaging, to a smaller or larger extent, into several courses, including Biological system modeling, Models in Biology and Epidemiology, Systems Biology, Traditional Medical and Ecological Imaging Systems and Imaging Systems with Nonionizing Radiation.

The research and teaching activity of the author in the field of perfusion imaging started in 2004 as a natural continuation of the cooperation with prof. Torfinn Taxt at University of Bergen, Norway, and his colleagues. The know-how in this field was gradually gained form the Norwegian partners and extended further, mainly in frame of research projects including colleagues from the Institute of Scientific Instruments of the Czech Academy of Sciences, Department of Biomedical Engineering at Brno University of Technology, the author's bachelor, master and doctoral students, as well as colleagues from the cooperating institutes.

The thesis is written as a collection of selected journal papers with an introduction. The introduction is meant as an explanation of the perfusion imaging field, starting with a general description, which is gradually narrowed down to ultrasound and magnetic-resonance (MR) perfusion imaging and their specifics. Furthermore, the focus is put on the specific topics where the author sees the main contribution of his group.

1 THEORY OF PERFUSION IMAGING

Most perfusion imaging methods, including the class of methods related to the focus of the author's group, are based on intravenous administration of a contrast agent and imaging of the tissue of interest before, during and after the administration. The recorded image sequence is subsequently processed. Contrast agents are sometimes referred to as indicators or tracers. The word indicator refers to a substance introduced into a physiological system that can be detected and give information about the system. A tracer is a type of indicator that has the same chemical structure as a systemic substance of interest [1].

For these techniques, the process of perfusion imaging can be divided into the following parts (Fig. 1):

- Data acquisition – acquisition of raw image data upon contrast-agent administration.
- Image-sequence reconstruction – reconstruction of an image sequence from the acquired raw image data.
- Preprocessing – e.g. motion correction due to cardiac and/or respiration, noise suppression.
- Conversion from image intensity to contrast-agent concentration.
- Extraction of contrast-agent concentration curves from the converted image sequence – for each voxel of interest or for each region of interest (ROI); in the following text, the term ROI will be used, without a loss of generality, for the case of single voxels or a set of voxels belonging to a presumably homogeneous tissue.
- Pharmacokinetic-model fitting – In quantitative perfusion-imaging methods, a pharmacokinetic model is then fitted to these contrast-agent concentration curves. The estimated parameters of the model and their combinations are the sought perfusion parameters of the given ROI (see Tab. 1.1 below for a list of perfusion parameters).
- Visualization, interpretation – e.g. perfusion-parameter maps overlaid over an anatomical image; followed by interpretation of the results, possibly classification.
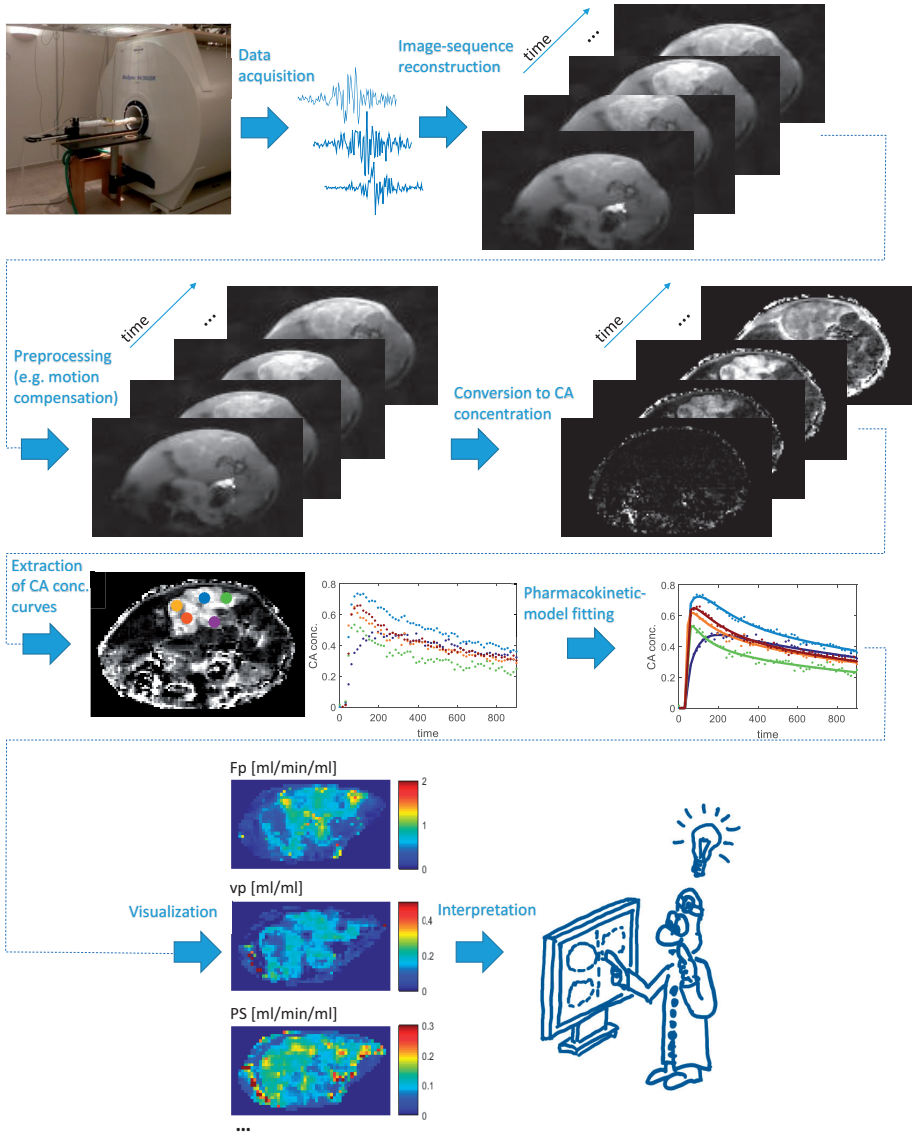
Fig. 1.1: Perfusion-imaging process. Example images from MR perfusion imaging of tumor-bearing mice, axial slice, tumor (hyper-intense contrast-agent-uptaking area in the upper right area of images) located in the flank of the hind limb.

Quantity	Description	Unit
F_p	Plasma flow	ml/min/ml
F_b	Blood flow	ml/min/ml
PS	Permeability-surface area product (measure of vessel-wall "leakiness" for the contrast agent)	ml/min/ml
v_p	Plasma volume	ml/ml
v_b	Blood volume	ml/ml
v_e	Volume of the extravascular extracellular space (EES)	ml/ml
E	Extraction fraction (fraction of contrast-agent particles that are extracted into the interstitium)	-
T_c	Capillary mean transit time (average time needed for a contrast-agent particle to pass through the perfusion unit)	min
K^{trans}	Volume transfer constant (compound parameter: $K^{trans} = EF_p$)	1/min
k_{ep}	Interstitium-to-plasma rate constant (compound parameter: $k_{ep} = EF_p/v_e$)	1/min
σ, α	Parameters describing the the statistical distribution of the capillary transit times (used in DCATH and GCTT models, σ, α capture the structure of the microvessels)	min, -
BAT	Bolus arrival time (delay between the global AIF and the local perfusion-unit-specific local AIF)	min

Tab. 1.1: Overview of the most usual perfusion parameters.

To narrow down the scope of this text, it is important to mention also perfusion-analysis methods that are not in focus of our work and will not be considered in the following sections. In one group of these methods, only so called semi-quantitative parameters of the contrast-agent concentration curves are estimated, without proper pharmacokinetic modeling of their course. Such semi-quantitative perfusion parameters are for example slope of the initial rising phase of the contrast-agent inflow or the area under the curve within some time window. Several semi-quantitative approaches to perfusion imaging are based on models of contrast-agent concentration curves that are fitted to the measured data. Some of these models might be denoted as pharmacokinetic models as they describe mathematically the physiology of the vascular system. For example the gamma-variate model [2, 3] is related to a series of compartments[1] that represent neighboring sections of the vascular system. Other such pharmacokinetic models are for example the lagged-normal [4, 3], the Local Density Random Walk (LDRW) and the First Passage Time (FPT) models [5, 3]. Use of these models is typical for perfusion imaging using ultrasonography. The problem of this approach is that they describe the shape of the contrast-agent bolus and the whole vascular system from the location of bolus administration to the tissue ROI. This means that the estimated parameters of these models depend not only on the tissue ROI but also on the bolus-administration procedure and on the physiology of the arterial tree proximal to the tissue ROI. This makes these methods hardly reproducible and comparable among different imaging centers.

An even more simplistic approach, falling also into the field of *perfusion imaging*, includes only the acquisition part. The acquired image sequence is then visually (subjectively) assessed without any modeling or estimation of semi-quantitative parameters.

Both the semi-quantitative and visual approaches are not in the focus of our work as they depend on the used contrast agent, its administration, the imaging device itself, the acquisition setup and the operator (in the latter case). The trend in modern medical imaging is to use an imaging device not as a "snapshot camera", but rather as a measuring apparatus that can measure selected biomarkers, in physical units, independently of the acquisition details and vendors of the used devices. Use of such user- and vendor-independent quantitative imaging methods minimizes the subjectivity of radiographer's decision and allows for multicentric studies. Thus, only the quantitative approaches (based on pharmacokinetic modeling allowing separation of the administered bolus shape and the properties of the proximal

---

[1]In pharmacokinetics, a compartment is an idealized well-mixed volume with homogeneous concentration of the observed substance.

arterial tree from the perfusion properties of the tissue ROI) have been in focus of our work, hence the name *quantitative* in the title of the thesis. Thus, the following text deals only with the quantitative perfusion imaging methods.

A plethora of perfusion imaging approaches exist. They vary based on

- the contrast-agent administration method (e.g. bolus, dual-bolus, infusion),
- imaging modality (e.g. positron emission tomography, computed tomography, MR imaging), the selected acquisition method and its setup,
- method for conversion from image intensity to contrast-agent concentration,
- pharmacokinetic model,
- approach to model fitting,
- other specifics related to the application, e.g. acquisition synchronized with cardiac and sometimes respiration activity, together with the subsequent image registration is needed for cardiac applications.

Perfusion imaging methods should not be confused with flow velocity imaging where blood velocity and flow is measured in big vessels using e.g. Doppler ultrasonography or MR velocity imaging techniques. In perfusion imaging, perfusion parameters are measured on the microvascular level the extents of which are far lower than the spatial resolution achievable with standard medical imaging modalities. The perfusion parameters refer to average quantities within the ROI (e.g. a voxel), for example average blood volume within the ROI.

1.1 Short history overview

Measuring of perfusion started in nuclear medicine in early 1960s as a preclinical (i.e. applicable to laboratory animals) measurement method. It was based on administration of radioactive microspheres (preferably by a catheter as a bolus into left atrium or left ventricle). After the first passage through the vasculature, the microspheres remained trapped in the arterioles or capillaries. Subsequently, the animals were sacrificed and tissue samples harvested. Then, the number of microspheres was measured using scintigraphy. [6, 7]

The first application of radiolabeled microspheres in man for assessment of perfusion was done in 1964 by Wagner et al. [8] where albumin-based microspheres were used for assessment of pulmonary blood flow. The radioactivity was originally detected by rectilinear scanners (a radiation detector physically moved over the surface of the patient), later replaced by gamma cameras in late 1960s.

From 1990s, use of radiolabeled microspheres in preclinical quantification of perfusion was partly substituted by use of fluorescent microspheres [9].

Perfusion imaging based on radiolabeled substances developed further. Planar imaging was replaced by tomographic imaging, namely by single-photon emission computed tomography (SPECT) and later by positron emission tomography (PET). For routine clinical practice, SPECT was introduced in the late 1980s [10]. PET imaging is a more expensive and technologically more complex imaging modality with shorter-lived and less easily obtainable radioisotopes than in SPECT imaging. PET has been considered to be a research tool for a long time. Compared to SPECT, PET provides higher spatial resolution and allows for smaller radioactive doses [11]. The most SPECT and PET perfusion imaging methods rely on static cumulative (uptake) images acquired after the radiotracer has accumulated in the tissue. In contrast to radiolabeled microspheres mentioned above, the SPECT/PET radiotracers do not accumulate intravascularly but extravasate and take part in metabolic changes in the cells [11].

Later, absolute quantification of blood flow has been pursued, especially using PET with the $H_2^{15}O$ tracer. This approach is based on dynamic imaging acquired before, during and after administration of the tracer and application of pharmacokinetic models to the acquired image sequences in the postprocessing step [12]. The pharmacokinetics-based $H_2^{15}O$ PET perfusion imaging has become gold standard in myocardial perfusion imaging [10, 11]. These pharmacokinetics-based techniques are closely related to the focus of the author's research group.

Computed Tomography (CT) perfusion imaging is based on intravenous administration of an iodinated contrast agent and dynamic CT scanning, followed by pharmacokinetic modeling of the acquired image sequences, similarly to $H_2^{15}O$ PET perfusion imaging mentioned above. The basics of CT perfusion imaging were laid down in 1979 [13] and 1980 [14] (before $H_2^{15}O$ PET perfusion imaging). However clinical application, mainly in acute-stroke and tumor patients, came much later.

Perfusion imaging in magnetic resonance is a term referring to several groups of methods. The first group is based on administration of an exogenous contrast agent, similarly to CT and PET/SPECT mentioned above. The most MR contrast agents are chelates of gadolinium. Their concentration is related to shortening of T_1, T_2 and T_2^* relaxation times. Depending on the measured relaxation time, the contrast-agent based methods are further categorized into *Dynamic Contrast-Enhanced (DCE) Magnetic Resonance Imaging (MRI)* (based on T_1-weighted image sequences) and *Dynamic Susceptibility Contrast-enhanced (DSC) MRI* (based on T_2- or T_2^*-weighted

image sequences).

The basics of DSC-MRI date back to late 1980th when Villringer at al. [15] used a gadolinium-based contrast agent on rats (in brain) and showed contrast-agent curves related to concentration and suggested their use for perfusion imaging. DSC-MRI on human became reality in the 1990th [16, 17, 18]. The main application of DSC-MRI has been stroke imaging where it provides, in combination with diffusion-weighted MRI, identification of the so called penumbra – the potentially salvageable brain tissue.

DCE-MRI started in early 90th, with applications in cardiology [19] (myocardium perfusion of an isolated rat's heart and of healthy human subjects in vivo), neurology [20, 21, 22] (assessment of blood-brain-barrier permeability in multiple-sclerosis and brain-tumor patients). The main domain of DCE-MRI has been tumor imaging.

Another group of MR-perfusion-imaging methods does not require application of any exogenous contrast agent. These methods rely on an endogenous contrast agent being blood. In this case, blood is labeled "magnetically" by the MR scanner's coil system, i.e. by a defined modification of the magnetic moment of the blood flowing to the regions of interest. These so called Arterial Spin Labeling (ASL) methods are known since 1992 [23] and have become very popular, partly also in the clinics in the recent decade. Another MR perfusion imaging method with no need for an exogenous contrast agent is the Intravoxel Incoherent Motion (IVIM) technique, known from 1986 [24]. It is related to diffusion MRI as blood flow mimics a water-molecule diffusion process. The ASL and IVIM techniques are out of the scope of this text.

Ultrasound perfusion imaging (Dynamic Contrast-Enhanced Ultrasonography – DCE-US) is also based on administration of an exogenous contrast agent. Ultrasound contrast agents are gas-filled microbubbles of the size of several micrometers. The contrast mechanisms have been known from 1968 [25]. Ultrasound contrast agents were commercially available since 1991 (Echovist, Bayer Shering Pharma AG). Nonlinear properties of microbubbles are used in various contrast imaging modes of ultrasonographs. The main domain of contrast agent use in ultrasonography is cardiology where it has been used for better delineation of the heart cavities. There are two main approaches in ultrasound perfusion imaging: bolus tracking and burst-replenishment.

Bolus-tracking methods are similar to the above mentioned $H_2^{15}O$ PET, CT and DCE/DSC-MRI perfusion imaging methods based on administration of a contrast-agent bolus. Bolus-tracking ultrasound perfusion imaging has been first used in

2000 for assessment of myocardial perfusion [26] and in brain perfusion [27].

Burst-replenishment methods assume continuous infusion of a contrast agent with intermittent applications of high-energy ultrasound pulses which destroy the microbubbles in the imaging plain. The following replenishment of the contrast agent is imaged and analyzed. Burst-replenishment ultrasound perfusion imaging has been first reported in 1998 for myocardial perfusion [28].

1.2   Basic pharmacokinetic models

In this section, pharmacokinetic modeling as the core of perfusion imaging will be shortly described. In pharmacokinetic modeling, a tissue ROI is treated as a perfusion unit with an arterial input, venous output and the microvascular segment in between (Fig. 1.2). Only tissue ROIs with small vessel size are assumed so that the vessels can be viewed as a statistical set of randomly organized structures [29]. This limits the vessel size to the maximum diameter of several hundreds μm, corresponding to small arteries, arterioles, capillaries [2], venules and small veins [30].
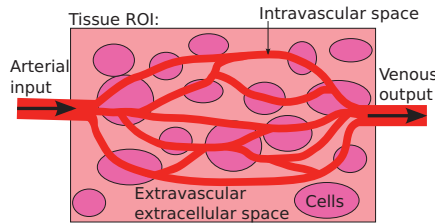

Fig. 1.2: Schematic of a perfusion unit assumed by pharmacokinetic models.

The ROI consists of the intravascular and the extravascular extracellular space (EES)[3] and the intracellular space. As this text is focused on ultrasonography- and MRI-based perfusion imaging, only the contrast agents used with these modalities will be considered further on. Ultrasound contrast agents remain only in the intravascular space, due to their large size on the order of micrometers, and do not diffuse through the vessel wall. Hence the term *non-diffusible contrast agents*. Thus, only the intravascular space needs to be modeled in this case.

---

[2]A specific case is DSC-MRI based on T_2-weighted acquisition which is sensitive predominantly to the signal from capillaries but not from larger vessels; this property is related to the nature of the acquisition process.

[3]This term is used in literature on perfusion imaging, although it is not accurate, as it could also include other volumes which are not captured by the pharmacokinetic models, such as lymphatic vessels, brain ventricles, etc. – the term interstitial space would be more appropriate.

On the other hand, MR contrast agents are much smaller and extravasate to the EES. Thus, MR contrast agents are referred to as *diffusible contrast agents*. It is also a known fact that MR contrast agents do not diffuse further into the cells. Hence, in MR perfusion imaging the intravascular space and the EES are modeled. An exception is brain imaging with intact blood brain barrier, which makes the vessel wall impermeable also for MR contrast agents. This is mostly the case of DSC-MRI in stroke.

A perfusion unit, described using a pharmacokinetic model, is assumed to be a linear stationary system [31]. An "input signal" of the modeled perfusion unit is the so called *Arterial Input Function* (AIF). It is the arterial input in Fig. 1.2, i.e. the time course of the contrast-agent concentration in the arterial input of the ROI. As the intravascular distribution volume, accessible to the contrast agent, is blood plasma, AIF is usually expressed as the contrast-agent concentration in plasma, $c_p(t)$. In the most perfusion imaging techniques, the AIF is assumed to be known, either from literature (population-based models) or from a measurement in some large artery (see below).

A straightforward interpretation of Fig. 1.2 assigns the output of the perfusion unit to the time course of the contrast-agent concentration in the venous output, $c_v(t)$. However, this signal is not accessible for measurement (as the size of these single draining vessels is far below the achievable spatial resolution). However, it is instructive to stay at this formulation of the system's output. In this case, the output is given as

$$c_v(t) = F_p(c_p * h)(t). \tag{1.1}$$

The scaling constant F_p is flow of blood plasma (defined as plasma flow per unit tissue volume), see Tab. 1.1 for overview of perfusion parameters. The symbol $*$ is time-domain convolution, The function $h(t)$ is the so called *transport function*. In the theory of systems, $h(t)$ is the perfusion-unit's impulse response function. Another interpretation of $h(t)$ is the probability distribution of contrast-agent-particle transit times. The expectation of $h(t)$ is the mean transit time of contrast-agent particles through the perfusion unit. The function $h(t)$ acts as a propagator through the perfusion unit. [31]

In perfusion imaging, the measured signal, i.e. the "output signal" of the perfusion unit, is the time course of the contrast-agent concentration within the tissue ROI, $c_t(t)$, not in its venous output $c_v(t)$. Hence, the impulse response of the perfusion unit is referred to as *Impulse Residue Function* (IRF), $R(t)$ [31], sometimes also called impulse response function. It is interpreted as the probability that the contrast-agent particle is present in the perfusion unit at time t following an instantaneous bolus of the contrast agent at the arterial input (Dirac-pulse AIF)

at time $t = 0$. From the definition, it follows that the IRF is a non-increasing function satisfying $R(t = 0) = 1$. It is related to the transport function as follows:

$$R(t) = 1 - \int_0^t h(\tau)d\tau. \tag{1.2}$$

The contrast-agent concentration within the tissue unit is then expressed as

$$c_t(t) = F_p(c_p * R)(t). \tag{1.3}$$

This is the basic pharmacokinetic model used in perfusion-imaging literature. The pharmacokinetic models differ based on the form of $R(t)$. In the following text, different formulations of the IRF, $R(t)$, will be reviewed. The perfusion parameters accessible using the different pharmacokinetic models are summarized in Tab. 1.2.

Model	Primary perfusion parameters	Derived perfusion parameters
	Non-diffusible models	
Nonparametric	F_p, v_p	T_c
Compartment	F_p, v_p	T_c
Plug-flow	F_p, v_p	T_c
	Diffusible models, 1st generation	
Tofts	K^{trans}, v_e	k_{ep}
Extended Tofts	K^{trans}, v_e, v_p	k_{ep}
Patlak	K^{trans}, v_p	-
	Diffusible models, 2nd generation	
2CX	F_p, v_p, v_e, PS	T_c, E, K^{trans}, k_{ep}
TH	F_p, v_p, v_e, PS	T_c, E, K^{trans}, k_{ep}
ATH	F_p, v_p, v_e, PS	T_c, E, K^{trans}, k_{ep}
DP	F_p, v_p, v_e, PS	T_c, E, K^{trans}, k_{ep}
DCATH	F_p, v_p, v_e, PS, σ	T_c, E, K^{trans}, k_{ep}
GCTT	F_p, v_p, v_e, PS, α	T_c, E, K^{trans}, k_{ep}

Tab. 1.2: Perfusion parameters estimated using different pharmacokinetic models. Primary perfusion parameters – one of possible choice of model parametrization (shows the number of unknown parameters of the given model), derived perfusion parameters – remaining perfusion parameters that can be derived from the primary perfusion parameters.

1.2.1 Models for non-diffusible contrast agents

Some perfusion-imaging methods are based on a nonparametric approach, where a non-parametric IRF is assumed [32]. According to the general pharmacokinetic

model (Eq. (1.3)), the measured tissue concentration curves, $c_t(t)$, are deconvolved with the AIF, $c_p(t)$, which yields an estimate of $F_p \cdot R(t)$. Regularization, such as Tikhonov regularization or truncated singular value decomposition, is sometimes used to deal with the ill-posedness of the deconvolution problem [33].

Then, F_p is estimated from $F_p \cdot R(t)$ as the first sample (because $R(t = 0) = 1$) or as its maximum. Plasma volume, v_p, (Tab. 1.1) is calculated as the ratio of areas under the tissue and AIF curves:
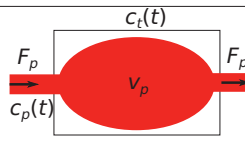
$$v_p = \frac{\int_0^{\inf} c_t(t)dt}{\int_0^{\inf} c_p(t)dt}. \tag{1.4}$$

The mean transit time, T_c, (Tab. 1.1) is derived from F_p and v_p according to the central volume principle [34] as

$$T_c = v_p/F_p. \tag{1.5}$$

Compared to non-parametric IRF, use of parametric IRF imposes additional assumptions about the perfusion unit, which can stabilize estimation of the perfusion parameters by limiting the set of possible solutions. This is however at the cost of decreased realism of the pharmacokinetic model because each IRF model brings a certain degree of simplification. The most broadly used parametric IRF models of the intravascular space (Tab. 1.3) are the compartment and plug-flow models. A compartment model describes the intravascular space as a well-mixed volume with a homogeneous contrast-agent concentration. Such model is suitable for a chaotic microvascular structure with no prevailing orientation of the vessels, such as the brain microvasculature for example. The dynamics of the contrast-agent distribution in a one-compartment perfusion unit can be described by a 1st-order ordinary differential equation. The solution leads to the convolutional model Eq. (1.3) with $R(t) = \exp(-t \cdot F_p/v_p)$ [35]. Fitting this model to the measured signal, $c_t(t)$, yields estimates of F_p and v_p (and T_c from the central volume principle).

A plug-flow model describes the microvasculature as a tube or a set of parallel tubes where all particles move with the same velocity. This relates to erythrocytes acting as "plugs" because they have a slightly larger size than the lumen of capillaries. When deformed erythrocytes are passing through the capillaries, they induce the same velocity of the plasma space between them. A plug-flow model is suitable for tissues with unidirectionally organized vessels, e.g. some muscle structures. The IRF of a plug-flow perfusion unit is $R(0 <= t <= T_c) = 1$ and $R(t) = 0$ elsewhere [35].

Compartment model	
• homogeneous contrast-agent concentration • exponential IRF	
Plug-flow model	
• constant speed of contrast-agent particles • boxcar IRF	
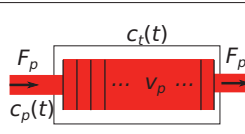
Tab. 1.3: Pharmacokinetic models for non-diffusible contrast agents.

1.2.2 Models for diffusible contrast agents

This section reviews pharmacokinetic models modeling the contrast-agent distribution within both the intravascular space and the EES. For these models, the approach of a non-parametric IRF has been used rarely [36]. In Eqs. (1.4), (1.5), the distribution volume, v_p, of the non-diffusible-contrast-agent case needs to be replaced by the distribution volume of the diffusible-contrast-agent case being $v_p + v_e$. The mean transit time, T_c, in Eq. (1.5) is replaced by the mean transit time of contrast-agent particles through the whole perfusion unit including the EES.

Parametric IRF models of diffusible contrast agents are of various degrees of complexity. As for the intravascular space, some models assume this space has negligible contribution and do not model it, e.g. the Tofts model [21, 37]. In the extended Tofts or the Patlak models, the intravascular signal is included but the structure of the intravascular space is not modeled (as it is irrelevant for the assumed high-flow conditions) [36]. These models are referred to as 1st-generation models (Tab. 1.4), dating back to the 1990s, where the quality of acquired MRI data was not sufficient to extract F_p, PS, T_c and E. This became possible later, with the so called 2nd-generation models, such as the 2CX, TH, ATH, DP, DCATH and GCTT models (see Tab. 1.5 for the full names, schematics and short descriptions). These models are based on a compartment or plug-flow model of the intravascular space and on a compartment or distributed-parameter model of the EES. The advantage of the 2nd-generation models is that they provide a more complete set of perfusion parameters than the 1st-generation models. For example the perfusion parameter K^{trans} provided by the 1st-generation models is affected by both plasma flow, F_p, and the permeability-surface area product, PS (describing the "leakiness" of the vessel wall for the contrast agent). Hence, the 1st-generation models do not allow differentiating the effects of blood flow and permeability. Separating the flow and permeability properties gives important information about the tissue

microvasculature state. This is provided by the 2nd-generation models. On the other hand, the 2nd-generation models are more complex and require better data quality.

A thorough description of the pharmacokinetic models is beyond the scope of this introduction. The reader can refer to several reviews on this topic [31, 36, 38].
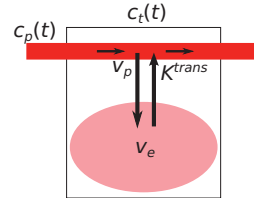
Tofts model
- only EES assumed
- EES modeled as a compartment
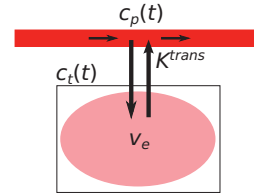
Extended Tofts model
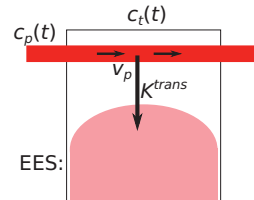- vascular signal considered
- structure of the intravascular space not modeled (high plasma flow assumed)

Patlak model
- vascular signal considered
- structure of the intravascular space not modeled (high plasma flow assumed)
- backflux from the EES to the vascular space neglected (uptake model)

Tab. 1.4: First-generation pharmacokinetic models for diffusible contrast agents.

2-Compartment eXchange (2CX) Model • intravascular space modeled as a compartment • EES modeled as a compartment	
Tissue-Homogeneity (TH) model • plug-flow model of the vascular space • EES modeled as a compartment • no analytic time-domain expression of the IRF, $R(t)$, only frequency-domain expression available	
Adiabatic approximation of the Tissue Homogeneity model (ATH) • plug-flow model of the vascular space • EES modeled as a compartment • assumption of much faster intravascular contrast-agent dynamics compared to the dynamics in the EES	
Distributed-Parameter (DP) model • plug-flow model of the vascular space • distributed model of the EES • contrast-agent exchange only between the corresponding intravascular-space and EES units • no exchange (diffusion) between the neighboring EES units assumed	
Distributed-Capillary Adiabatic Tissue Homogeneity (DCATH) and Gamma Capillary Transit Time (GCTT) models • as the ATH model but multiple intravascular paths with different transit times assumed • additional perfusion parameter describing the statistical distribution of the mean capillary transit times	

Tab. 1.5: Second-generation pharmacokinetic models for diffusible contrast agents.

1.3 Main problems

Perfusion imaging using MRI and ultrasonography have been known since the 1980th / late 1990th. However, in the most clinical applications, current perfusion imaging methods are not sufficiently reliable for routine clinical use, where they remain mostly at the experimental level. Due to the vast variability of the available methods and due to their poor reproducibility among different scanners and scanner setups, there is a lack of standardization of the perfusion-imaging procedures. The situation is even worse in preclinical use, with a substantially smaller number of users, and hence lower business profit and interest of the scanner vendors.

One exception, in MRI, is DSC-MRI in stroke patients. Although the majority acute stroke examinations are made using CT, DSC-MRI is an officially approved standardized option, used in advanced medical imaging centers.

The Main reasons for the prevailing experimental character of perfusion imaging with MR and ultrasonography can be summarized as follows.

- There is still a dominating tendency to use simplistic semi-quantitative methods where the estimated perfusion parameters depend on the contrast-agent administration, on the properties of the proximal arterial system of the patient and on the scanner and its setup.

  This clearly leads to the need for fully quantitative perfusion imaging methods. These methods model the shape of the contrast-agent bolus entering the analyzed tissue ROI (perfusion unit), i.e. the AIF, which captures the influence of the contrast-agent administration process and the influence of the arterial tree proximal to the tissue ROI. This means that the convolutional model (Eq. (1.3)) needs to be the model of choice in quantitative perfusion imaging.

- Related to the previous point is the need for accurate estimation of the AIF. The AIF is commonly considered equal for all voxels of the examined tissue (global AIF). In most studies, it is measured (extracted from the acquired image sequence) in a big artery or taken as a parametric population-based AIF from literature. In MRI, the measured AIF is distorted by flow artifacts, partial volume effects, saturation, T_2^* effects and dispersion of the contrast-agent bolus between the AIF measurement location and the examined tissue. In DCE-US, deriving the AIF from an arterial ROI in the measured image sequence is an even more problematic task than in MRI, mainly due to attenuation of the contrast agent (dependent on the contrast-agent concentration, i.e. changing throughout the acquisition time). In addition, similar problems as in DCE-MRI arise: motion artifacts, low spatial resolution, blood-velocity dependence of the backscattered signal and dispersion of the contrast-agent bolus.

On the other hand, use of a population-based AIF, as another possibility to determine the AIF, ignores the differences in the vascular tree between different individuals and depends on the acquisition protocol and the contrast-agent-administration procedure used when these "standard" AIFs were established.

- In DCE-MRI, still mostly 1st-generation pharmacokinetic models are used. As mentioned above, they provide ambiguous information concerning the common parameters K^{trans} and k_{ep} which mix together the effects of plasma flow and vessel wall permeability without a chance to distinguish between them. Furthermore, these models are too simplistic for many tissue types and lead to biased perfusion-parameter estimates.

  A solution is to use more complex, 2nd-generation, models. However this leads to higher demands on the temporal resolution and signal-to-noise ratio (SNR), often ill-conditioned model fitting and higher sensitivity to the accuracy and precision of the AIF. Hence these models are still not much used.

2 CONTRIBUTION OF THE AUTHOR'S TEAM

The general aim of our group concerning both ultrasound and MRI perfusion imaging was and is to contribute to reliable quantitative perfusion analysis that gives accurate perfusion parameters independent of the contrast-agent-administration procedure, image-data acquisition methods and their setup, and the subject-specific properties of the arterial tree proximal to the ROI. Achieving this helps to bring ultrasound and MRI perfusion imaging closer to routine clinical practice and improve the diagnostics in many clinical and preclinical applications.

In the following text, our contribution is described more specifically, split into items. In most cases, an item corresponds to 1 or 2 journal paper(s) (co)authored by our group, possibly accompanied by our related conference contributions. The main journal papers, constitute attachments of the habilitation thesis.

2.1 Ultrasound perfusion imaging

The author believes that his group has contributed to introduction of quantitative perfusion imaging into DCE-US to replace the semi-quantitative methods. As pointed out earlier, the majority of DCE-US was done in a semi-quantitative manner.

The burst-replenishment DCE-US method is a semi-quantitative approach by nature, unless the parameters of the replenishment-curve model are scaled with respect to the arterial signal (as an analogy to the AIF in the bolus-tracking methods). To the author's knowledge, at the publication time of our first papers in DCE-US [39, 40, 41] (2010-2013), there were only three papers of two groups on quantitative burst-replenishment DCE-US (with normalization with respect to the arterial signal) [42, 43, 44], all applied to cardiac perfusion imaging.

A similar situation was present in bolus-tracking DCE-US. To the author's knowledge, at the publication time of our first papers in DCE-US there were two papers of one group [45, 46] using the convolution model Eq. (1.3) for estimation of the mean transit time, T_c, and slightly later, in 2012, another group published a convolution-based approach where all three available perfusion parameters were estimated (T_c, F_b, v_b) [47, 48].

The main contribution of our group in the field of DCE-US can be summarized as follows.

- We have introduced deconvolution-based perfusion imaging to bolus-tracking DCE-US and validated the methodology on a flow phantom [39, 49] and on pig's heart [50].

- We have newly formulated the standard burst-replenishment DCE-US method, using the convolutional formalism (i.e. using the convolution model Eq. (1.3)). This made it possible to combine the burst-replenishment approach with deconvolution-based bolus-tracking. In this combined approach, we called *Bolus & Burst*, the contrast agent is administered as a bolus and image data recorded as in the bolus-tracking method, but in addition, during the same image-recording session a high-energy burst is applied in the later slow-dynamics phase. Simultaneous processing of the bolus and replenishment signals leads to more robust perfusion analysis than processing of the bolus or replenishment signals alone. Having the bolus and replenishment signals interconnected through the convolutional model represents sufficient information to estimate the AIF together with the IRF (parametrized by the sought perfusion parameters T_c, F_b, v_b). This approach is called blind deconvolution – "blind" because both components of the convolution (Eq. (1.3)) are unknown. This approach avoids the problems connected to measuring the AIF or using population-based AIFs (see above). The author considers the *Bolus & Burst* method as the core of our contribution in DCE-US. We have published the methodology paper as [40] (*Paper I* of this habilitation thesis).
- We have extended our original *Bolus & Burst* method with a more accurate model [51]. In [41] (*Paper II* of this habilitation thesis), we have validated this extended *Bolus & Burst* method on clinical data from Crohn's disease patients where we have shown that it could be used as a treatment-stratification method for patients with Crohn's disease, particularly to distinguish between inflammatory and fibrous wall thickening of the gastrointestinal tract.
- The *Bolus & Burst* method was further tested on patients with exocrine pancreatic failure [52]. Interobserver agreement for repeated recordings using the same ultrasound scanner and agreement between results on two different scanner systems were evaluated.
- Another successful validation study of the *Bolus & Burst* method was done on patients with insufficiency of pancreas related to cystic fibrosis and on healthy volunteers [53].
- The *Bolus & Burst* processing chain was further extended by automatic compensation of motion using translational and non-rigid image registration with a temporal continuity assumption [54].
- We have further developed the *Bolus & Burst* method by implementing new AIF models suitable for DCE-US of small animals [55, 56] and illustrated the method on tumor-bearing mice and compared the results with DCE-MRI [57], all presented so far as conference proceedings papers.

2.2 MR perfusion imaging

In MR, convolution-based quantitative perfusion imaging has been more common than in ultrasonography. The main focus of our group has been DCE-MRI. Here, the most widely used pharmacokinetic models are the 1st-generation models, such as the Tofts and extended Tofts models. Our contribution was towards reliable DCE-MRI based on 2nd-generation models.

Our main effort was focused on accurate estimation of the AIF, which avoids the problems connected to measured or population-based AIFs. The main approach, similarly to our DCE-US work, was blind deconvolution, where both the IRF and AIF are estimated from the measured tissue concentration curves. Blind-deconvolution estimation of the AIF was proposed by the group of Edward DiBella (Univ. of Utah, USA) [58, 59, 60], with applications in DCE-MRI using 1st-generation pharmacokinetic models. At approximately the same time, the group of Torfinn Taxt (Univ. of Bergen, Norway) introduced blind-deconvolution AIF estimation into DSC-MRI [61, 62, 63]. Having a close cooperation with Torfinn Taxt and his group (and later partly with DiBella's group), we have built on this work. Together with Torfinn Taxt and his colleagues, we have applied blind-deconvolution AIF estimation to DCE-MRI using 2nd-generation pharmacokinetic models. Use of 2nd-generation models is more sensitive to the accuracy of AIF estimation and presents a more difficult problem than use of the 1st-generation models.

The main contribution of our group in DCE-MRI can be summarized as follows. Estimation of the AIF using blind deconvolution:

- We have proposed blind-deconvolution AIF estimation method with 2nd-generation pharmacokinetic models and a nonparametric AIF [64, 65] and validated them on DCE-MRI recordings from mice with induced muscle inflammation.

- DCE-MRI data processing and analysis based on blind deconvolution from the previous point was the core of our part in two major preclinical studies on tumor-bearing rats and the effects of antiangiogenic treatment with bevacizumab [66, 67]. The experimental setup and analysis methods, including our perfusion-imaging methodology, have revealed new insights into the physiological background of the treatment processes.

- We have further extended the above mentioned blind-deconvolution AIF estimation to use a semi-parametric AIF (initial rapidly changing part of the AIF was left nonparametric, while the "tail" was mathematically modeled), leading to more accurate AIF estimates [68]. The method was validated on recordings from mice with induced muscle inflammation.

- We have also contributed to blind-deconvolution AIF estimation with fully parametric AIF models to further constrain the AIF estimation process (used in connection with 2nd-generation pharmacokinetic models). In [69] (*Paper III* of this habilitation thesis), we have proposed such method for clinical DCE-MRI and validated it on renal-cell-carcinoma patients. In [70] (*Paper IV* of this habilitation thesis), we have proposed such method with an AIF model tailored to small-animal DCE-MRI and validated it within a study on tumor-bearing mice.

- the above mentioned blind deconvolution method with semi-parametric AIF was applied on a longitudinal preclinical study where the time development of bevacizumab's effects was studied at several time points during the treatment [71] (*Paper V* of this habilitation thesis). With our perfusion-imaging methodology we have contributed to gain new insights into the dynamics of the treatment effect.

Other topics:

- We have proposed a new estimation scheme for an advanced 2nd-generation model (DCATH) with a continuous formulation of all perfusion parameters, including the bolus arrival time, thanks to its estimation in the frequency domain [72]. This allows us to use standard gradient-based optimization algorithms in pharmacokinetic-model fitting of the tissue concentration time sequences. In addition to perfusion parameters, we have estimated also their confidential intervals. We have newly proposed a method for estimation of the confidential intervals of the perfusion parameters derived from the primary ones parametrizing the IRF.

- To increase the robustness of DCE-MRI with 2nd-generation models, we have incorporated spatial regularization into pharmacokinetic-model fitting. Hence, the model-fitting process was not done separately for each voxel, as usual, but simultaneously for all voxels with induced similarity of the neighboring voxels, based on the (edge-preserving) total variation (TV) regularization [73], (*Paper VI* of this habilitation thesis).

3   CONCLUSIONS

Our main contribution to ultrasound and MRI perfusion imaging was in fully quantitative perfusion analysis, as a means of reliable measurement of perfusion biomarkers, reproducible across different imaging scanners and differences in their acquisition setup (and independent of patient-specific arterial-tree properties). We have been pursuing the idea of treating ultrasonography and MRI not only as an imaging tool but rather as measuring devices.

In this respect, our main contribution in DCE-US was introducing a novel method, *Bolus & Burst*, which combines the bolus tracking and burst-replenishment methods, both formulated using convolution-based pharmacokinetic models. The perfusion-analysis process is performed using blind deconvolution which avoids the need for measurement of the AIF. This makes *Bolus & Burst* robust with respect to estimation errors due to AIF-measurement artifacts.

In DCE-MRI, we have followed the same idea of avoiding the need to measure the AIF by the use of blind-deconvolution, with a special focus on the use of 2nd-generation pharmacokinetic models, where the requirements on the accuracy and precision of AIF estimates are higher than for the more commonly used 1st-generation pharmacokinetic models. We have also contributed to improved reliability of perfusion analysis using 2nd-generation pharmacokinetic models by proposing a proper continuous formulation of the pharmacokinetic model and by introducing edge-preserving spatial regularization into the perfusion analysis.

The topic of perfusion analysis has been the core of several successfully defended bachelor, diploma and Ph.D. theses led by the author and several related theses led by his colleagues. The topic of perfusion imaging has been also introduced into several courses at Brno University of Technology, Dept. of Biomedical Engineering.

Our work in the field of quantitative perfusion analysis brought us in closer contact with broader national and international scientific community, often thanks to our long-term cooperation with Torfinn Taxt from University of Bergen, Norway. Our cooperation with the Institute of Medicine, University of Bergen, Norway and the National Centre of Ultrasound in Gastroenterology at Haukeland University Hospital, Bergen, Norway (Odd Helge Gilja, Kim Nylund, Trond Engjom) has been very fruitful in sense of validation of our DCE-US *Bolus & Burst* method on actual clinical applications. Our cooperation with the Department of Biomedicine, University of Bergen, Bergen, Norway (Rolf Bjerkvig, Eskil Eskilsso, Nina Obad) and the Luxembourg Institute of Health (Olivier Keunen) has helped us to apply our MR perfusion-analysis methods to actual problems in search for antiangiogenic cancer treatment. Finally, we have also started active cooperation with the group of

Edward DiBella, University of Utah, USA, in the field of DCE-MRI of myocardium [74]. This field represents a challenge due to complicated acquisition connected to cardiac and respiratory motion and it is one of our future orientations.

The increasing number of interested users of our perfusion-imaging methods has brought us to development of an online tool for perfusion analysis, called PerfLab `http://perflab.cerit-sc.cz/`, currently implemented as a prototype version. It is designed as a web-based database of studies, datasets and batches of perfusion analyses, providing a step-by-step perfusion analysis of DCE-US and DCE-MRI data. The web-based graphical user interface guides the user in entering the processing parameters, drawing ROIs, plotting of their concentration curves, browsing through the image sequences in each processing step and previewing of the resulting perfusion maps. The web-based character of PerfLab avoids the need for installation of any software, except for the web browser. For clinical users, the data can be imported through the service ReDiMed (`https://www.medimed.cz/en/redimed`) directly from the radiology workstation. Import of the DCE-US/DCE-MRI data is available for several clinical and preclinical scanners. PerfLab has been partly tested by our colleagues at the University of Bergen, Luxembourg Institute of Health and Stanford University. Our further development of this online software tool is directed towards thorough evaluation on clinical and preclinical data, dissemination and possibly future research and/or commercial use.

The current research focus of our group extends the above described work in several directions. First, we have implemented modern compressed-sensing DCE-MRI acquisition schemes based on sparse data sampling and spatially regularized image-sequence reconstruction to overcome the limits of standard MRI acquisition given by the Nyquist theorem [75, 76]. This approach provides increased spatial and/or temporal resolution or improved spatial coverage of the organ of interest. The spatial-regularization term can also be learned using modern deep-learning approaches, to provide even higher efficiency of the acquisition/reconstruction process which is a further natural extension of the compressed-sensing techniques.

On the level of applications (of DCE-MRI), the above described perfusion-analysis methodology becomes more challenging when applied in cardiology and stroke imaging, where we intend to extend our know-how and hopefully contribute to the current state of the art. In cardiology, the main challenge is to synchronize the data acquisition process with the cardiac and respiratory motion while acquiring enough data for reliable image reconstruction and subsequent perfusion analysis. In stroke imaging, the main challenge is the low SNR of DCE-MRI data due to the blood brain barrier (preventing the contrast agent from extravasation) but allows quantification of subtle blood-brain-barrier disruption [77, 78].

BIBLIOGRAPHY

[1] N. A. Lassen, W. Perl, W. A. Perl, Tracer Kinetic Methods in Medical Physiology, Raven Press, 1979.

[2] T. HK, S. CF, W. RE, M. HD, INDICATOR TRANSIT TIME CONSIDERED AS A GAMMA VARIATE, Circulation research 14 (1964) 502–515. `doi:10.1161/01.RES.14.6.502`.

[3] C. Strouthos, M. Lampaskis, V. Sboros, A. Mcneilly, M. Averkiou, Indicator dilution models for the quantification of microvascular blood flow with bolus administration of ultrasound contrast agents, IEEE Transactions on Ultrasonics, Ferroelectrics, and Frequency Control 57 (6) (2010) 1296–1310. `doi:10.1109/TUFFC.2010.1550`.

[4] J. B. Bassingthwaighte, F. H. Ackerman, E. H. Wood, Applications of the Lagged Normal Density Curve as a Model for Arterial Dilution Curves, Circulation Research 18 (4) (1966) 398–415. `doi:10.1161/01.RES.18.4.398`.

[5] M. MISCHI, Z. D. PRETE, H. H. M. KORSTEN, INDICATOR DILUTION TECHNIQUES IN CARDIOVASCULAR QUANTIFICATION, 2007, pp. 89–155. `doi:10.1142/9789812771377_0004`.

[6] M. A. Heymann, B. D. Payne, J. I. Hoffman, A. M. Rudolph, Blood flow measurements with radionuclide-labeled particles, Progress in Cardiovascular Diseases 20 (1) (1977) 55–79. `doi:10.1016/S0033-0620(77)80005-4`.

[7] H. N. Wagner, B. A. Rhodes, Y. Sasaki, J. P. Ryan, Studies of the circulation with radioactive microspheres (1969). `doi:10.1097/00004424-196911000-00004`.

[8] H. N. Wagner, D. C. Sabiston, M. Iio, J. G. Mcafee, J. K. Meyer, J. K. Langan, Regional Pulmonary Blood Flow in Man by Radioisotope Scanning, JAMA: The Journal of the American Medical Association 187 (8) (1964) 601–603. `doi:10.1001/jama.1964.03060210051012`.

[9] G. RW, B. S, B. M, Validation of fluorescent-labeled microspheres for measurement of regional organ perfusion, Journal of applied physiology (Bethesda, Md. : 1985) 74 (5) (1993) 2585–2597. `doi:10.1152/JAPPL.1993.74.5.2585`.

[10] A. Notghi, C. S. Low, Myocardial perfusion scintigraphy: past, present and future`doi:10.1259/bjr/14625142`.

[11] R. S. Driessen, P. G. Raijmakers, · . Wijnand, J. Stuijfzand, · . P. Knaapen, Myocardial perfusion imaging with PET, The International Journal of Cardiovascular Imaging 33 (2017) 1021–1031. `doi:10.1007/s10554-017-1084-4`.

[12] S. V. Nesterov, C. Han, M. Mäki, S. Kajander, A. G. Naum, H. Helenius, I. Lisinen, H. Ukkonen, M. Pietilä, E. Joutsiniemi, J. Knuuti, J. Knuuti, S. V. Nesterov, M. Mäki, A. G. Naum, H. Helenius, H. Ukkonen, M. Pietilä, . E. Joutsiniemi, Myocardial perfusion quantitation with 15 O-labelled water PET: high reproducibility of the new cardiac analysis software (Carimasâ„˘), Eur J Nucl Med Mol Imaging 36 (2009) 1594–1602. `doi:10.1007/s00259-009-1143-8`.

[13] H. R. Heinz, P. Dubois, D. Osborne, B. Drayer, W. Barrett, Dynamic Computed Tomography Study of the Brain, Journal of Computer Assisted Tomography 3 (5) (1979) 641–649. `doi:10.1155/2015/397521`.

[14] L. Axel, Cerebral blood flow determination by rapid-sequence computed tomography. A theoretical analysis, Radiology 137 (3) (1980) 679–686. `doi:10.1148/radiology.137.3.7003648`.

[15] A. Villringer, B. R. Rosen, J. W. Belliveau, J. L. Ackerman, R. B. Lauffer, R. B. Buxton, Y. S. Chao, V. J. Wedeenand, T. J. Brady, Dynamic imaging with lanthanide chelates in normal brain: Contrast due to magnetic susceptibility effects, Magnetic Resonance in Medicine 6 (2) (1988) 164–174. `doi:10.1002/mrm.1910060205`.

[16] R. R. Edelman, H. P. Mattle, D. J. Atkinson, T. Hill, J. P. Finn, C. Mayman, M. Ronthal, H. M. Hoogewoud, J. Kleefield, Cerebral blood flow: Assessment with dynamic contrast-enhanced T2*-weighted MR imaging at 1.5 T, Radiology 176 (1) (1990) 211–220. `doi:10.1148/radiology.176.1.2353094`.

[17] B. R. Rosen, J. W. Belliveau, B. R. Buchbinder, R. C. McKinstry, L. M. Porkka, D. N. Kennedy, M. S. Neuder, C. R. Fisel, H. J. Aronen, K. K. Kwong, R. M. Weisskoff, M. S. Cohen, T. J. Brady, Contrast agents and cerebral hemodynamics, Magnetic Resonance in Medicine 19 (2) (1991) 285–292. `doi:10.1002/mrm.1910190216`.

[18] S. Warach, J. F. Dashe, R. R. Edelman, Clinical outcome in ischemic stroke predicted by early diffusion-weighted and perfusion magnetic resonance imaging: A preliminary analysis, Journal of Cerebral Blood Flow and Metabolism 16 (1) (1996) 53–59. `doi:10.1097/00004647-199601000-00006`.

[19] D. J. Atkinson, D. Burstein, R. R. Edelman, First-pass cardiac perfusion: Evaluation with ultrafast MR imaging (1990). `doi:10.1148/radiology.174.3.2305058`.

[20] H. B. Larsson, M. Stubgaard, J. L. Frederiksen, M. Jensen, O. Henriksen, O. B. Paulson, Quantitation of blood-brain barrier defect by magnetic resonance imaging and gadolinium-DTPA in patients with multiple sclerosis and brain tumors, Magnetic Resonance in Medicine 16 (1) (1990) 117–131. `doi:10.1002/mrm.1910160111`.

[21] P. S. Tofts, A. G. Kermode, Measurement of the blood brain barrier permeability and leakage space using dynamic MR imaging. 1. Fundamental concepts, Magnetic Resonance in Medicine 17 (2) (1991) 357–367. `doi:10.1002/mrm.1910170208`.

[22] G. Brix, W. Semmler, R. Port, L. R. Schad, G. Layer, W. J. Lorenz, Pharmacokinetic parameters in cns gd-dtpa enhanced mr imaging, Journal of Computer Assisted Tomography 15 (4) (1991) 621–628.

[23] J. A. Detre, J. S. Leigh, D. S. Williams, A. P. Koretsky, Perfusion imaging, Magnetic Resonance in Medicine 23 (1) (1992) 37–45. `doi:10.1002/mrm.1910230106`.

[24] D. Le Bihan, E. Breton, D. Lallemand, P. Grenier, E. Cabanis, M. Laval-Jeantet, MR imaging of intravoxel incoherent motions: Application to diffusion and perfusion in neurologic disorders, Radiology 161 (2) (1986) 401–407. `doi:10.1148/radiology.161.2.3763909`.

[25] R. Gramiak, P. M. Shah, Echocardiography of the Aortic Root, Investigative Radiology 3 (5) (1968) 356–366.

[26] J. R. Lindner, F. S. Villanueva, J. M. Dent, K. Wei, J. Sklenar, S. Kaul, Assessment of resting perfusion with myocardial contrast echocardiography: Theoretical and practical considerations, American Heart Journal 139 (2) (2000) 231–240. `doi:10.1016/S0002-8703(00)90231-X`.

[27] M. Wiesmann, G. Seidel, Ultrasound perfusion imaging of the human brain, Stroke 31 (10) (2000) 2421–2425. `doi:10.1161/01.STR.31.10.2421`.

[28] K. Wei, A. R. Jayaweera, S. Firoozan, A. Linka, D. M. Skyba, S. Kaul, Quantification of myocardial blood flow with ultrasound-induced destruction

of microbubbles administered as a constant venous infusion, Circulation 97 (5) (1998) 473–483. `doi:10.1161/01.CIR.97.5.473`.

[29] V. G. Kiselev, On the theoretical basis of perfusion measurements by dynamic susceptibility contrast MRI, Magnetic Resonance in Medicine 46 (6) (2001) 1113–1122. `doi:10.1002/mrm.1307`.

[30] N. Herring, Levick's introduction to cardiovascular physiology, sixth edition.. Edition, 2018.

[31] S. P. Sourbron, D. L. Buckley, Tracer kinetic modelling in MRI: estimating perfusion and capillary permeability, Physics in Medicine and Biology 57 (2) (2011) R1–R33. `doi:10.1088/0031-9155/57/2/R1`.

[32] L. Østergaard, ISMRM Perfusion Workshop Invited Paper Principles of Cerebral Perfusion Imaging by Bolus Tracking (2005). `doi:10.1002/jmri.20460`.

[33] S. Sourbron, R. Luypaert, P. V. Schuerbeek, M. Dujardin, T. Stadnik, Choice of the regularization parameter for perfusion quantification with MRI, Physics in Medicine & Biology 49 (14) (2004) 3307. `doi:10.1088/0031-9155/49/14/020`.

[34] P. Meier, K. L. Zierler, On the Theory of the Idcator-Dihtion Method for Meawwement of Blood Flow md Volzmel.

[35] L. Østergaard, R. M. Weisskoff, D. A. Chesler, C. Gyldensted, B. R. Rosen, High resolution measurement of cerebral blood flow using intravascular tracer bolus passages. Part I: Mathematical approach and statistical analysis, Magnetic Resonance in Medicine 36 (5) (1996) 715–725. `doi:10.1002/MRM.1910360510`.

[36] S. P. Sourbron, D. L. Buckley, Classic models for dynamic contrast-enhanced MRI., NMR in biomedicine 26 (8) (2013) 1004–27. `doi:10.1002/nbm.2940`.

[37] P. S. Tofts, G. Brix, D. L. Buckley, J. L. Evelhoch, E. Henderson, M. V. Knopp, H. B. Larsson, T. Y. Lee, N. A. Mayr, G. J. Parker, R. E. Port, J. Taylor, R. M. Weisskoff, Estimating kinetic parameters from dynamic contrast-enhanced T1-weighted MRI of a diffusable tracer: Standardized quantities and symbols., JMRI 10 (3) (1999) 223–32.

[38] T. S. Koh, S. Bisdas, D. M. Koh, C. H. Thng, Fundamentals of tracer kinetics for dynamic contrast-enhanced MRI, Journal of Magnetic Resonance Imaging 34 (6) (2011) 1262–1276. `doi:10.1002/jmri.22795`.

[39] M. Mézl, R. Jiřík, V. Harabiš, R. KoláĹ™, Quantitative ultrasound perfusion analysis in vitro, ANALYSIS OF BIOMEDICAL SIGNALS AND IMAGES, Proceedings of Biosignal (2010) 279–283.

[40] R. Jiřík, K. Nylund, O. H. Gilja, M. Mézl, V. Harabiš, R. Kolá, M. Standara, T. Taxt, Ultrasound Perfusion Analysis Combining Bolus-Tracking and Burst-Replenishment, IEEE Transactions on Ultrasonics, Ferroelectrics, and Frequency Control 60 (2) (2013) 310–319.

[41] K. Nylund, R. Jiřík, M. Mézl, S. Leh, T. Hausken, F. Pfeffer, S. Ødegaard, T. Taxt, O. H. Gilja, Quantitative Contrast-Enhanced Ultrasound Comparison Between Inflammatory and Fibrotic Lesions in Patients with Crohn's Disease, Ultrasound in Medicine & Biology 39 (7) (2013) 1197–1206. doi:10.1016/j.ultrasmedbio.2013.01.020.

[42] R. Vogel, A. Indermuhle, J. Reinhardt, P. Meier, P. T. Siegrist, M. Namdar, P. A. Kaufmann, C. Seiler, The quantification of absolute myocardial perfusion in humans by contrast echocardiography: Algorithm and validation, Journal of American College of Cardiology 45 (5) (2005) 754–762.

[43] T. Rutz, S. F. de Marchi, M. Schwerzmann, R. Vogel, C. Seiler, Right ventricular absolute myocardial blood flow in complex congenital heart disease, Heart 96 (13) (2010) 1056–1062.

[44] H. Komatsu, S. Yamada, H. Iwano, M. Okada, H. Onozuka, T. Mikami, S. Yokoyama, M. Inoue, S. Kaga, M. Nishida, C. Shimizu, K. Matsuno, H. Tsutsui, Angiotensin II receptor blocker, valsartan, increases myocardial blood volume and regresses hypertrophy in hypertensive patients, Circulation Journal 73 (11) (2009) 2098–2103.

[45] P. C. Li, C. K. Yeh, S. W. Wang, Time-intensity-based volumetric flow measurements: An in vitro study, Ultrasound in Medicine and Biology 28 (3) (2002) 349–358. doi:10.1016/S0301-5629(01)00516-6.

[46] P. C. Li, M. J. Yang, Transfer function analysis of ultrasonic time-intensity measurements, Ultrasound in medicine & biology 29 (10) (2003) 1493–1500. doi:10.1016/S0301-5629(03)00968-2.

[47] M. Gauthier, F. Tabarout, I. Leguerney, M. Polrot, S. Pitre, P. Peronneau, N. Lassau, Assessment of Quantitative Perfusion Parameters by Dynamic Contrast-Enhanced Sonography Using a Deconvolution Method An In Vitro and In Vivo Study, Journal of Ultrasound in Medicine 31 (2012) 595–608.

[48] M. Gauthier, S. Pitre-Champagnat, F. Tabarout, I. Leguerney, M. Polrot, N. Lassau, Impact of the arterial input function on microvascularization parameter measurements using dynamic contrast-enhanced ultrasonography., World journal of radiology 4 (7) (2012) 291–301. `doi:10.4329/wjr.v4.i7.291`.

[49] M. Mézl, R. Jiřík, V. Harabiš, R. Kolář, M. Standara, K. Nylund, O. H. Gilja, T. Taxt, Absolute ultrasound perfusion parameter quantification of a tissue-mimicking phantom using bolus tracking, IEEE Transactions on Ultrasonics, Ferroelectrics, and Frequency Control 62 (5) (2015) 983–987. `doi:10.1109/TUFFC.2014.006896`.

[50] M. Mézl, R. Jiřík, K. Matre, K. Grong, P.-R. Salminen, M. T. Lonnebakken, T. Taxt, Quantitative myocardial perfusion analysis with contrast-enhanced ultrasound bolus tracking - preliminary animal results, in: 2013 IEEE International Ultrasonics Symposium (IUS), IEEE, 2013, pp. 541–544. `doi:10.1109/ULTSYM.2013.0140`.

[51] R. Jiřík, K. Nylund, T. Taxt, M. Mézl, T. Hausken, V. Harabiš, R. Kolář, M. Standara, O. H. Gilja, Parametric ultrasound perfusion analysis combining bolus tracking and replenishment, in: 2012 IEEE International Ultrasonics Symposium, IEEE, 2012, pp. 1323–1326. `doi:10.1109/ULTSYM.2012.0330`.

[52] M. Stangeland, T. Engjom, M. Mézl, R. Jiřík, O. H. Gilja, G. Dimcevski, K. Nylund, Interobserver Variation of the Bolus-And-Burst Method for Pancreatic Perfusion with Dynamic-Contrast-Enhanced Ultrasound, Ultrasound International Open 3 (3) (2017) E99–E106. `doi:10.1055/s-0043-110475`.

[53] T. Engjom, K. Nylund, F. Erchinger, M. Stangeland, B. Lærum, M. Mézl, R. Jiřík, O. Gilja, G. Dimcevski, Contrast-enhanced ultrasonography of the pancreas shows impaired perfusion in pancreas insufficient cystic fibrosis patients, BMC Medical Imaging 18 (1) (2018). `doi:10.1186/s12880-018-0259-3`.

[54] S. Schäfer, K. Nylund, F. Sævik, T. Engjom, M. Mézl, R. Jiřík, G. Dimcevski, O. H. Gilja, K. Tönnies, Semi-automatic motion compensation of contrast-enhanced ultrasound images from abdominal organs for perfusion analysis., Computers in biology and medicine 63 (2015) 229–37. `doi:10.1016/j.compbiomed.2014.09.014`.

[55] M. Mézl, R. Jiřík, K. Souček, R. Kolář, Evaluation of accuracy of bolus and burst method for quantitative ultrasound perfusion analysis with various

arterial input function models, 2015 IEEE International Ultrasonics Symposium (IUS) (1) (2015) 1–4. `doi:10.1109/ULTSYM.2015.0482`.

[56] M. Mézl, R. Jiřík, L. Dvořáková, E. Dražanová, R. Kolář, Comparison of arterial input function models for small-animal ultrasound perfusion imaging, in: IEEE International Ultrasonics Symposium, IUS, Vol. 2016-Novem, 2016. `doi:10.1109/ULTSYM.2016.7728503`.

[57] R. Jiřík, K. Souček, M. Mézl, M. Bartoš, E. Dražanová, F. Dráfi, L. Grossová, J. Kratochvíla, O. Macíček, K. Nylund, A. Hampl, O. H. Gilja, T. Taxt, Z. Starčuk, Blind deconvolution in dynamic contrast-enhanced MRI and ultrasound., in: Conf Proc IEEE Eng Med Biol Soc., Vol. 2014, Institute of Electrical and Electronics Engineers Inc., 2014, pp. 4276–9. `doi:10.1109/EMBC.2014.6944569`.

[58] D. Y. Riabkov, E. V. R. D. Bella, Estimation of Kinetic Parameters Without Input Functions : Analysis of Three Methods for Multichannel Blind Identification, IEEE T Bio-Med Eng 49 (11) (2002) 1318–1327.

[59] J. U. Fluckiger, M. C. Schabel, E. V. R. DiBella, Model-Based Blind Estimation of Kinetic Parameters in Dynamic Contrast Enhanced (DCE)-MRI, Magnetic Resonance in Medicine 62 (6) (Dec. 2009).

[60] M. C. Schabel, J. U. Fluckiger, E. V. R. DiBella, A model-constrained Monte Carlo method for blind arterial input function estimation in dynamic contrast-enhanced MRI: I. Simulations, Physics in Medicine and Biology 55 (16) (2010) 4783–4806.

[61] G. R, T. T, Iterative blind deconvolution in magnetic resonance brain perfusion imaging, Magnetic resonance in medicine 55 (4) (2006) 805–815. `doi:10.1002/MRM.20850`.

[62] R. Grü, B. T. Bjørnarå, G. Moen, T. Taxt, Magnetic Resonance Brain Perfusion Imaging With Voxel-Specific Arterial Input Functions, J. Magn. Reson. Imaging 23 (2006) 273–284. `doi:10.1002/jmri.20505`.

[63] R. Grü, T. Taxt, Cepstral Estimation of Arterial Input Functions in Brain Perfusion Imaging, J. Magn. Reson. Imaging 26 (2007) 773–779. `doi:10.1002/jmri.21115`.

[64] T. Taxt, R. Jiřík, C. B. Rygh, R. Gruner, M. Bartos, E. Andersen, F. R. Curry, R. K. Reed, Single-Channel Blind Estimation of Arterial Input Function

and Tissue Impulse Response in DCE-MRI, IEEE Transactions on Biomedical Engineering 59 (4) (2012) 1012–1021. `doi:10.1109/TBME.2011.2182195`.

[65] T. Taxt, T. Pavlin, R. K. Reed, F.-R. Curry, E. Andersen, R. Jiřík, Using Single-Channel Blind Deconvolution to Choose the Most Realistic Pharmacokinetic Model in Dynamic Contrast-Enhanced MR Imaging, Applied Magnetic Resonance 46 (6) (2015) 643–659. `doi:10.1007/s00723-015-0679-y`.

[66] O. Keunen, M. Johansson, A. Oudin, M. Sanzey, S. A. A. Rahim, F. Fack, F. Thorsen, T. Taxt, M. Bartos, R. Jiřík, H. Miletic, J. Wang, D. Stieber, L. Stuhr, I. Moen, C. B. Rygh, R. Bjerkvig, S. P. Niclou, Anti-VEGF treatment reduces blood supply and increases tumor cell invasion in glioblastoma, Proceedings of the National Academy of Sciences 108 (9) (2011) 3749–3754. `doi:10.1073/pnas.1014480108`.

[67] E. Eskilsson, G. Rosland, K. Talasila, S. Knappskog, O. Keunen, A. Sottoriva, S. Foerster, G. Solecki, T. Taxt, R. Jirik, S. Fritah, P. Harter, K. Välk, J. Al Hossain, J. Joseph, R. Jahedi, H. Saed, S. Piccirillo, I. Spiteri, L. Leiss, P. Euskirchen, G. Graziani, T. Daubon, M. Lund-Johansen, P. Enger, F. Winkler, C. Ritter, S. Niclou, C. Watts, R. Bjerkvig, H. Miletic, EGFRvIII mutations can emerge as late and heterogenous events in glioblastoma development and promote angiogenesis through Src activation, Neuro-oncology 18 (12) (2016).

[68] T. Taxt, R. K. Reed, T. Pavlin, C. B. Rygh, E. Andersen, R. Jiřík, Semi-parametric arterial input functions for quantitative dynamic contrast enhanced magnetic resonance imaging in mice, Magnetic Resonance Imaging 46 (2018) 10–20. `doi:10.1016/J.MRI.2017.10.004`.

[69] J. Kratochvíla, R. Jiřík, M. Bartoš, M. Standara, Z. Starčuk, T. Taxt, Distributed capillary adiabatic tissue homogeneity model in parametric multi-channel blind AIF estimation using DCE-MRI, Magn Reson Med 75 (3) (2016) 1355–1365. `doi:10.1002/mrm.25619`.

[70] R. Jiřík, T. Taxt, O. Macíček, M. Bartoš, J. Kratochvíla, K. Souček, E. Dražanová, L. Krátká, A. Hampl, Z. Starčuk, Blind deconvolution estimation of an arterial input function for small animal DCE-MRI, Magnetic Resonance Imaging 62 (2019) 46–56. `doi:10.1016/J.MRI.2019.05.024`.

[71] N. Obad, H. Espedal, R. Jiřík, P. O. Sakariassen, C. Brekke Rygh, M. Lund-Johansen, T. Taxt, S. P. Niclou, R. Bjerkvig, O. Keunen, Lack of functional

normalisation of tumour vessels following anti-angiogenic therapy in glioblastoma, Journal of Cerebral Blood Flow & Metabolism 38 (10) (2018) 1741–1753. `doi:10.1177/0271678X17714656`.

[72] M. Bartoš, R. Jiřík, J. Kratochvíla, M. Standara, Z. Starčuk, T. Taxt, The precision of DCE-MRI using the tissue homogeneity model with continuous formulation of the perfusion parameters., Magnetic resonance imaging 32 (5) (2014) 505–13. `doi:10.1016/j.mri.2014.02.003`.

[73] M. Bartoš, P. Rajmic, M. Šorel, M. Mangová, O. Keunen, R. Jiřík, Spatially regularized estimation of the tissue homogeneity model parameters in DCE-MRI using proximal minimization, Magnetic Resonance in Medicine 82 (6) (2019) 2257–2272. `doi:10.1002/mrm.27874`.

[74] R. Jiřík, J. Mendes, Y. Tian, G. Adluru, E. Dibella, Hybrid Estimation of the Arterial Input Function Using Blind Deconvolution and the Measured Blood Pool Signal, in: ISMRM Proceedings 2018, 2018, p. 2965.

[75] M. Mangová, P. Rajmic, R. Jiřík, Dynamic magnetic resonance imaging using compressed sensing with multi-scale low rank penalty, in: 2017 40th International Conference on Telecommunications and Signal Processing, TSP 2017, Vol. 2017-Janua, 2017. `doi:10.1109/TSP.2017.8076094`.

[76] R. Jiřík, M. Marie, P. Rajmic, O. Macíček, K. Souček, Z. Starčuk, Advanced pharmacokinetic modeling in small-animal compressed-sensing DCE-MRI, in: ESMRMB 2019 Congress, Elsevier, Rotterdam, 2019, pp. S346–S348. `doi: 10.1007/s10334-019-00755-1`.

[77] R. Jiřík, M. Marie, P. Rajmic, L. Krátká, L. Dvořáková, E. Dražanová, Z. Starčuk, Absolute Quantification of Brain Perfusion using Golden Angle Compressed Sensing DCE-MRI, in: ISMRM Proceedings 2017, 2017, p. 6400.

[78] R. Jiřík, L. Krátká, J. Kratochvíla, O. Macíček, Y. Tian, P. Scheer, J. Hložková, M. Bartoš, E. DiBella, Z. Starčuk, Blood Flow and Permeability Imaging in a Rat Stroke Model Using 3D Compressed-Sensing DCE-MRI, in: ISMRM Proceedings 2020, 2020, p. 3771.

Abstract

The habilitation thesis summarizes the contribution of the author's team to the field of perfusion imaging in ultrasonography and magnetic resonance imaging. First, the general concept of these perfusion-imaging approaches is described. Then, a short history overview of perfusion imaging is given and put in context of other medical imaging modalities. Subsequently, the used pharmacokinetic models are described. Finally, the main problems of the field are revised and the approach of the author's team to these problems is presented.

Abstrakt

Tato habilitační práce shrnuje přínos autorovy výzkumné skupiny k oblasti zobrazování perfuse pomocí ultrasonografie a magnetické resonance. Nejdříve je popsán celkový koncept těchto metod. Potom je krátce shrnut jejich historický vývoj a zasazen do kontextu ostatních zobrazovacích modalit. Následně jsou popsány používané farmakokinetické modely. Nakonec jsou shrnuty hlavní problémy této oblasti a je presentován přístup autorova týmu k jejich řešení.